EDGE ARTICLE

Check for updates

All publication charges for this article have been paid for by the Royal Society of Chemistry

Abiotic formation of hexoses and disaccharides in aqueous microdroplets†

Myles Quinn Edwards, Dylan T. Holden [iD] and R. Graham Cooks [iD] *

Understanding the chemical reactions that led to the origin of life is a fundamental challenge of chemistry. The formose reaction, an abiotic pathway to monosaccharides, provides a mechanism of sugar formation from simple aldehydes and ketones. However, the reaction requires the addition of base, metal catalysts, and is prone to side reactions, leaving questions about how such processes could have occurred on a primitive Earth. The abiotic formation of more complex sugars, such as disaccharides also require catalysts, and remains underexplored compared to other classes of biomolecules. This study investigates the role of microdroplets in the formation of hexoses and their subsequent condensation reactions to produce disaccharides, without the need for catalysts. The microdroplet-mediated synthesis of fructose and sorbose from glyceraldehyde or dihydroxyacetone, as well as that of disaccharides from various pentoses or hexoses, was monitored *via* mass spectrometery. Products were confirmed by high resolution mass spectrometry and tandem mass spectrometry. The product distribution of glucose disaccharides was determined by matching the relative intensities of product ions to a mixture of six disaccharide and showed a maximum yield of 9.4% or 1.7 μg min^{-1} emitter. This study demonstrates the abiotic formation of monosaccharides and disaccharides, such as xylobiose and maltose, providing a possible link between prebiotic sugar synthesis and extant carbohydrate biochemistry. Hexose formation and disaccharide synthesis are driven by the unique air water interface of microdroplets, where partial solvation, pH extremes, and fast mass transfer kinetics enable abiotic transformations.

Introduction

Carbohydrates are fundamental to life on Earth, having essential roles as energy sources, signaling molecules, and structural components.[1-3] Understanding the formation of complex carbohydrates and their precursors under abiotic conditions provides insight into the mosaic of molecules that existed at life's origins and sustained its evolution.[3,4]

The formose reaction, discovered by Butlerov in 1861,[5] has been proposed as a critical pathway in primordial chemistry.[6,7] This reaction converts formaldehyde into an array of sugars, primarily through aldol addition reactions, condensation reactions, and isomerization. Key intermediates formed during the autocatalytic cycle,[8,9] including the trioses dihydroxyacetone and glyceraldehyde, contribute to the diversity of synthesized carbohydrates. Downstream products of the reaction, glycolaldehyde and dihydroxyacetone, have been detected in the interstellar medium,[10-12] as well as on the Murchison meteorite alongside sugars like ribose and xylose.[13,14] However, the formose reaction has significant limitations as a pathway for sugar

synthesis: it requires the addition of base to create alkaline conditions with divalent metal catalysts to proceed at an appreciable rate and prolonged exposure to reactive conditions leads to a mixture of products, often at the expense of the desired sugar products.[15] Nevertheless, any monosaccharides produced, such as glucose and xylose, can readily form disaccharides when treated with dilute acid.[16-19] Acidic wet-dry cycling of glucose has been shown to produce disaccharides as well as higher oligosaccharides, highlighting a plausible prebiotic pathway for carbohydrate oligomerization.[20] Yet, despite their potential importance in the formation and propagation of life during early chemical evolution,[3] the emergence of oligosaccharides on primordial earth has been overlooked relative to studies on nucleic acids[21-23] and peptides.[24,25]

Given these challenges, it is of interest to explore alternative chemical environments that could facilitate carbohydrate formation and oligomerization on early Earth. One such environment is sea spray aerosols. Formed by breaking waves and bursting air bubbles, these entities range in size from hundreds of nanometers to tens of micrometers and strongly influence atmospheric chemistry and climate.[26] In addition, Enceladus' cryovolcanic plumes, which eject water and ice,[27] represent an extraterrestrial analogue where the unique properties of small water aerosols may also be of astrobiological relevance, offering insights into the potential for life beyond Earth.[27-29]

Department of Chemistry, Purdue University, 560 Oval Drive, West Lafayette, 47907, USA. E-mail: Cooks@purdue.edu

† Electronic supplementary information (ESI) available. See DOI: https://doi.org/10.1039/d4sc08402k

Recent research has highlighted aqueous microdroplets as chemical environments capable of accelerating chemical reactions and driving reactions not normally favorable in bulk solution.[30–32] These microdroplets, present unique surface characteristics that can dramatically accelerate reaction kinetics[33–36] allowing them to serve as individual reaction vessels.[37,38] Reaction acceleration is a consequence of partial solvation of molecules at the air–water interface,[39,40] the strongly acidic and basic double layer,[33,34,41–44] a high interfacial electric field[45] and enhanced mass transfer.[46] The hydrophobic air–water interface provides a practical solution to the "water paradox" of life,[47] facilitating essential abiotic condensation reactions that produce peptides,[30,48,49] sugar phosphates,[50] ribonucleosides and ribonucleotides,[50–53] as well as phospholipids.[54]

In this study, the formation of sugars, both monosaccharides and disaccharides, is investigated using accelerated reactions in aqueous microdroplets. Specifically, the reactions of dihydroxyacetone and glyceraldehyde to produce sorbose and fructose, and the reactivity of both pentoses and hexoses to form disaccharides, are explored using online MS analysis.

Experimental

Materials

Liquid chromatography-MS-grade water (Fisher Scientific) was utilized for all experiments. D-Glucose-fructose, D-galactose, β-gentiobiose, D-arabinose, D-maltose monohydrate, D-trehalose, D-cellobiose, D-xylose, D-glyceraldehyde, dihydroxyacetone (all ≥98% purity) were purchased from Sigma-Aldrich. D-Sorbose, D-galactose, D-ribose (all ≥99% purity) and 2,4,6-trimethylpyrylium tetrafluoroborate (98+%) were purchased from Thermo-Fisher Scientific. Isomaltose (98.8% purity) was purchased from Santa Cruz Biotechnology. Nigerose (95% purity) was purchased from Megazyme. Kojibiose was purchased from Biosynth. 1,4-D-Xylobiose (98% purity) was purchased from A2B Chem. Sodium chloride (≥99.0% purity) was purchased from Avantor. All reagents and solvents were used as received. The final concentration of all chemicals was 10 mM unless otherwise noted.

Methods

nESI tips were made from borosilicate glass capillaries (Sutter Instrument Co.; outer diameter [O.D.] of 1.5 mm, inner diameter [I.D.] 0.86 mm) pulled to *ca.* 5 μm O.D. using a Flaming/Brown micropipette puller (P-97, Sutter Instrument Co). Solutions were ionized with ±2 kV spray potential supplied by the mass spectrometer to a platinum electrode placed inside the nESI capillary. The sonic spray ionization (SSI) spray emitter was constructed using fused silica lines with 250 μm I.D. and 360 μm O.D., as well as 50 μm I.D. and 160 μm O.D. (PolyMicro), one tee assembly, one union assembly, two NanoTight sleeves, and a silica capillary (IDEX Health and Science). To maintain the flow of reagent solution at a rate of 10 μL min^{-1}, syringe pumps (Standard Infusion PHD 22/2000, Harvard Apparatus)

were utilized with gastight syringes (Hamilton Robotics). N$_2$ was used as the nebulizing gas at 120 psi (Fig. S1†).

All disaccharide ion trap collision-induced dissociation (IT-CID) tandem mass spectrometry (MS/MS) experiments were performed using an LTQ ion trap mass spectrometer (Thermo Scientific) (ESI Note 1†).

High-resolution mass measurements (HRMS) on the products of pentose and hexose disaccharide synthesis were made using an LTQ-XL ion trap coupled with an Orbitrap mass spectrometer (Thermo Scientific). For analysis of the hexose reaction products, a modified Sciex TripleTOF 5600 quadrupole time-of-flight mass spectrometer was used.[55] Low-amplitude single-frequency excitation CID was performed on ions of m/z 179 for 30–50 ms in Q1 to remove noncovalent adducts before the resulting covalent products were fragmented at higher energy in Q2 and sent to the ToF for mass analysis. In all cases, helium was used as collision gas. To distinguish between covalent products and possible non-covalent clusters, the above technique for disrupting non-covalent interactions was used for the Q-ToF instrument. For an analogous method performed on the ion trap instrument, see ESI Note 2.†

Electrospray ionization (ESI) of 10 mM dihydroxyacetone and glyceraldehyde in water was performed in negative mode on an LTQ Orbitrap XL (Fig. S2–S4†). Additional control ESI experiments were conducted for 10 mM xylose and glucose, both in negative and positive modes (Fig. S5–S8†).

Results and discussion

Microdroplet production

Drawing inspiration from natural phenomena, microdroplets were generated using nano-electrospray ionization (nESI) and sonic spray ionization (SSI) (Fig. S1†) allowing for online characterization of chemical reactions by MS. Electrospray ionization is known to create a plume of charged droplets upon the application of an external potential to a liquid[56] with a range of droplet sizes from 10–40 μm.[57] Nano-electrospray ionization is a low flow version of electrospray ionization that uses smaller tip diameters to produce finer sprays of smaller charged microdroplets known to be 200 nm to 1 μm in size.[58,59] In contrast, sonic spray ionization generates small droplets by nebulizing a liquid sample with a high-velocity gas stream, creating a fine mist of charged microdroplets without the need for external high voltages.[60,61] Alongside other droplet production methods, both nESI and SSI methods have been shown the capability to produce microdroplets in which reactions are greatly accelerated.[30,62]

Hexose formation

Negative mode nESI was used to investigate the microdroplet chemistry of two trioses, dihydroxyacetone and glyceraldehyde. A peak at m/z 179 was observed in the full scan nESI spectra of both glyceraldehyde and dihydroxyacetone (Fig. S9–S11†). The high-resolution mass spectra revealed that the mass error for these peaks fell within 5 ppm of the value of a deprotonated hexose (Table S1†). Furthermore, a gentle collisional activation
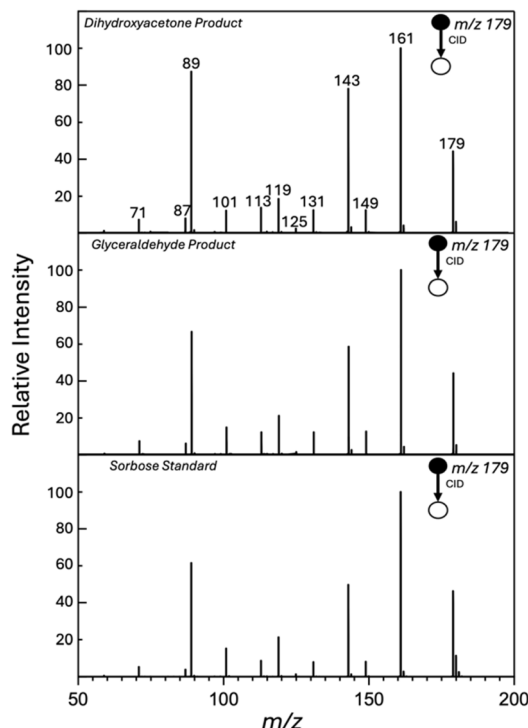
Fig. 1 Q-ToF tandem mass spectra of ions m/z 179 formed from various compounds. (Top) MS/MS fragmentation of m/z 179 ions from dihydroxyacetone. (Middle) MS/MS fragmentation of m/z 179 ions from glyceraldehyde. (Bottom) MS/MS fragmentation of the m/z 179 ions generated from authentic sorbose.

method prior to MS/MS was used to distinguish covalently bound ions from complexes (see Experimental) suggested the peak to primarily consist of the former and not the deprotonated noncovalent dimer $[C_3H_6O_3^- \cdots H^+ \cdots C_3H_6O_3^-]^-$. Authentic sorbose and fructose were used as reference compounds given that they are known products of the base-catalyzed reaction of glyceraldehyde and dihydroxyacetone.[63] MS/MS spectra showed that the ions at m/z 179 fragmentation in all cases (Fig. 1 and S12†) undergoes neutral losses of water and formaldehyde with the fragmentation patterns aligning with the known fragmentation behaviour of carbohydrates (ESI Note 3†).[64–67] In fact, the MS/MS spectra of the products formed from both dihydroxyacetone and glyceraldehyde closely match those of sorbose and fructose (Fig. 1 and S12†) indicating that both reaction products are present as a mixture.
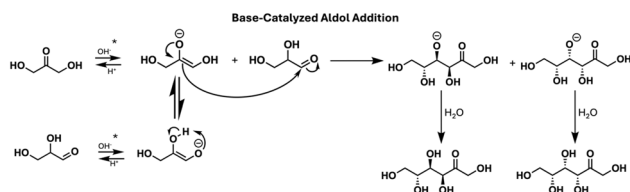
Scheme 1 Base-catalyzed aldol addition of dihydroxyacetone to glyceraldehyde to form the hexoses sorbose and fructose. The OH⁻ and H⁺ species are thought to be present in the microdroplet double layer. The asterisk (*) indicates keto–enol tautomerization, a process known to have enhanced rates in aqueous microdroplets.[70]

It is known that aldol reactions are accelerated in microdroplets.[68,69] Microdroplets have also been shown to accelerate keto–enol tautomerization.[70] This reversible process, where a ketone or aldehyde converts to an enol, is critical for aldol addition reactions, with the enolate acting as nucleophile in the base catalyzed version (Scheme 1). In addition, glyceraldehyde and dihydroxyacetone, may interconvert through the Lobry de Bruyn–Van Ekenstein transformation, under acidic or basic conditions.[71] While acidic catalysis is possible (ESI Note 4, Scheme S1†), a negative potential was applied and we primarily attribute hexose synthesis from dihydroxyacetone and glyceraldehyde to base-catalyzed aldol addition made possible by the pH extremes in the electric double layer containing a basic core augmented by partial solvation of the reagents at the surface[33,36,43,72] (Scheme 1).

To probe the effect of droplet size on the reaction, ESI data were compared to nESI data. For dihydroxyacetone with ESI, no peak at m/z 179 was present while the ESI spectrum of glyceraldehyde showed this peak but its fragmentation did not match that of hexose (Fig. S2–S4†). These experiments indicate that hexose was not formed during conventional (large droplet) ESI and that smaller droplets are needed to accelerate hexose formation, in line with literature precedence on accelerated reactions in microdroplets.[64]

Pentose disaccharide formation

Given the evidence for formation of hexoses in microdroplets, further investigations were conducted to determine if monosaccharides could react to form disaccharides. Using negative mode nESI HRMS to investigate the reactions of xylose, a peak at nominal m/z 281 was noted with the formula of deprotonated pentose disaccharide, $[C_{10}H_{18}O_9 - H]^-$ within 5 ppm mass error (Table S2†). However, the relative intensity of the species at m/z 281 was too low to provide meaningful fragmentation data. To produce more abundant ion populations, positive mode nESI was used with sodium chloride added to the stock solution to generate sodium-adducted pentose cations. While trace amounts of sodium cationized species were already present, likely due to sodium contamination from the solvent and glassware,[73] the deliberate addition of NaCl improved the signal intensity significantly. The full mass scan showed the sodium-bound monomer $[C_5H_{10}O_5 + Na]^+$, an ammonium adduct of the monomer $[C_5H_{10}O_5 + NH_4]^+$, the sodium-bound dimer $[C_5H_{10}O_5 + Na + C_5H_{10}O_5]^+$ as well as the putative sodium adducted pentose disaccharide $[C_{10}H_{18}O_9 + Na]^+$ (Fig. S13†). HRMS of this last ion agreed with the assignment of a sodiated pentose disaccharide (Table S2†).

In-source fragmentation can be used to distinguish covalent products from noncovalent gas-phase adducts.[74] In-source fragmentation was used to confirm the formation of a droplet synthesized covalent disaccharide product (ESI Note 2 and ESI Fig. S13†). Tandem MS of the suspected pentose disaccharide ions revealed characteristic fragmentation patterns of disaccharides,[75–77] including glycosidic bond cleavages on both the reducing and nonreducing units (Fig. 2). These fragmentation pathways, which also involve cross-ring cleavages, are
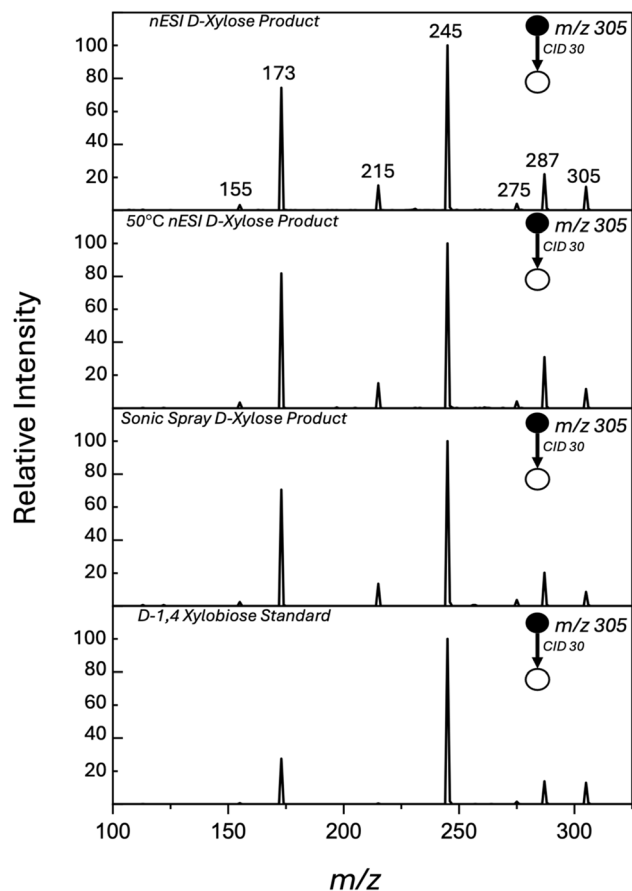
Fig. 2 MS/MS of ions m/z 305 formed from 10 mM aqueous xylose solution using typical nESI conditions, mass-selected in an ion trap and fragmented by collision-induced dissociation (CID 30, manufacturers unit) (Top panel); compared to 50 °C capillary nESI (2nd panel); using sonic spray instead of nESI (3rd panel); compared to ions generated from authentic pentose disaccharide 1,4-D-xylobiose (bottom panel).

consistent with previously reported data for pentose disaccharides (ESI Note 5†).[76]

To examine the effects of temperature and applied potential, additional experiments were performed using nESI with a low inlet temperature of 50 °C and also with sonic spray ionization. For both conditions, ions at m/z 305 were found at lower relative intensities as well as lower overall signal intensities compared to the standard nESI methodology yet produced similar fragmentation patterns (Fig. 2). No disaccharide ions were detected in either the positive or negative mode when using ESI (Fig. S5 and S6†) and this is again ascribed to the smaller reaction acceleration in the larger ESI droplets.

When other pentose monosaccharides (D-ribose, D-arabinose) were reacted in microdroplets, the disaccharide ion (m/z 305) gave the same fragment ions albeit with significantly different relative intensities suggesting the microdroplet promoted formation of pentose disaccharides is not unique to xylose (Fig. S14†).

The fragmentation of 1,4-D-xylobiose standard is shown in Fig. 2. The relative intensities of certain fragment products for the microdroplet produced disaccharide differ significantly

from the 1,4-D-xylobiose standard. For example, the ion at m/z 215 is at a consistent relative intensity of 20% for the xylose microdroplet product but is around 1% relative intensity of the 1,4-D-xylobiose standard. Given that this reaction utilizes an unprotected sugar and there are a variety of reactive sites on the monosaccharide, a distribution of disaccharide products is expected. The dominant products produced are likely the disaccharides with 1,4 linkages, which has been observed in previous bulk studies.[16,18] The similarity between the fragmentation patterns of the 1,4-D-xylobiose standard and the reaction product supports this conclusion. The likely preferred product of the two 1,4 linkages would be the α-1,4 linkage due to the anomeric effect stabilizing the reducing end in the axial position.[78] It is also probable that the mixture contains other linkages, such as the α-1,3 and α-1,2 linkages, based on findings from analogous studies in bulk.[16,18] The lack of standards and dearth of studies on the production of xylose disaccharides limits the characterization of the abundance of each disaccharide isomer. Thus, to further examine the mixture, the most well-characterized monosaccharide, glucose, was used to generate disaccharides and elucidate the complex mixture of products produced.

Hexose disaccharide formation

Glucose, subjected to positive ion mode nESI, yields adducts with ammonium $[C_6H_{12}O_6 + NH_4]^+$, sodium-adduct $[C_6H_{12}O_6 + Na]^+$, and potassium $[C_6H_{12}O_6 + K]^+$, and a sodium bound dimer $[C_{12}H_{22}O_{11} + Na]^+$ in addition to a peak at m/z 365 (Fig. S15†). The exact mass of the peak at m/z 365 matched the disaccharide sodium adduct $[C_{12}H_{22}O_{11} + Na]^+$ (Table S2†). Parenthetically, a peak was noted in the corresponding negative ion spectrum with an exact mass that corresponds to deprotonated disaccharide $[C_{12}H_{22}O_{11} - H]^-$ (Table S2†). However, as was the case for pentose disaccharides, the peak intensity was too low to allow MS/MS-based structural elucidation. Again, no peaks corresponding to a disaccharide were detected in either mode when examining larger droplets formed by conventional ESI (Fig. S7 and S8†). In-source fragmentation was used to determine whether the suspected disaccharide peak represented a covalent product, or a gas-phase adduct. The findings confirm the synthesis of a covalent product in the droplet environment (ESI Note 2 and ESI Fig. S15†).

MS/MS of the glucose product (m/z 365) revealed a fragmentation pattern which included neutral losses of diols and triols, as well as glycosidic bond and cross-ring cleavages, characteristic of sodium-bound hexose disaccharides (ESI Note 6†).[64,67,75,79] Experiments exploring the effects of temperature and applied potential, as was done for the pentose disaccharides confirm disaccharide formation by the microdroplet reaction rather than from the heated MS inlet or by application of an external potential Fig. 3A. The fragment peaks produced from the glucose product matched known disaccharide standards[64] however the intensities of the peaks do not. Moreover, when D-sorbose, D-fructose, and D-galactose were used to form disaccharides (m/z 365), MS/MS showed the same ions but with

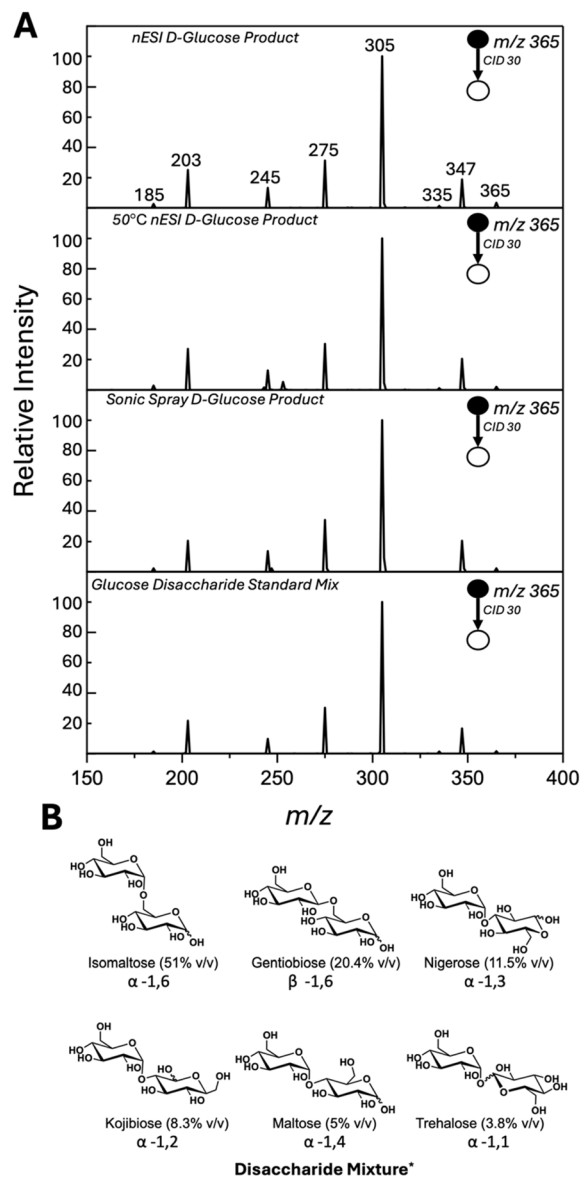Fig. 3   (A) MS/MS of ions of *m/z* 365 generated by nESI or sonic spray of glucose, mass selected in an ion trap and fragmented at CID 30 (manufacturers unit). (Top) Typical nESI conditions; (2nd panel) nESI with 50 °C inlet capillary; (3rd panel) sonic spray ionization; (Bottom) for disaccharide mixture. (B) Structures and volume fractions of disaccharides used in the disaccharide mixture. *Disaccharide standard mixture based on ref. 80.

Fig. 4   (A) Breakdown curve of the *m/z* 365 ions from the 10 mM glucose disaccharide mixture shown in Fig. 3B. (B) Breakdown curve of the ion of *m/z* 365 from the 10 mM glucose experiment.

differing intensities from the glucose mixture indicating the formation of multiple products (Fig. S16†).

Given the extreme pH known to be present at the microdroplet interface,[33] we compared the products generated from glucose droplet reactions to those generated from a non-enzymatic glycosylation reaction of glucose in an acidic lithium bromide trihydrate system,[80] an inorganic ionic liquid that might in some ways parallel the water deficient and acidic environment of a microdroplet interface. The top and bottom panel of Fig. 3A show the remarkable agreement between the fragmentation of the glucose reaction product and the mixture
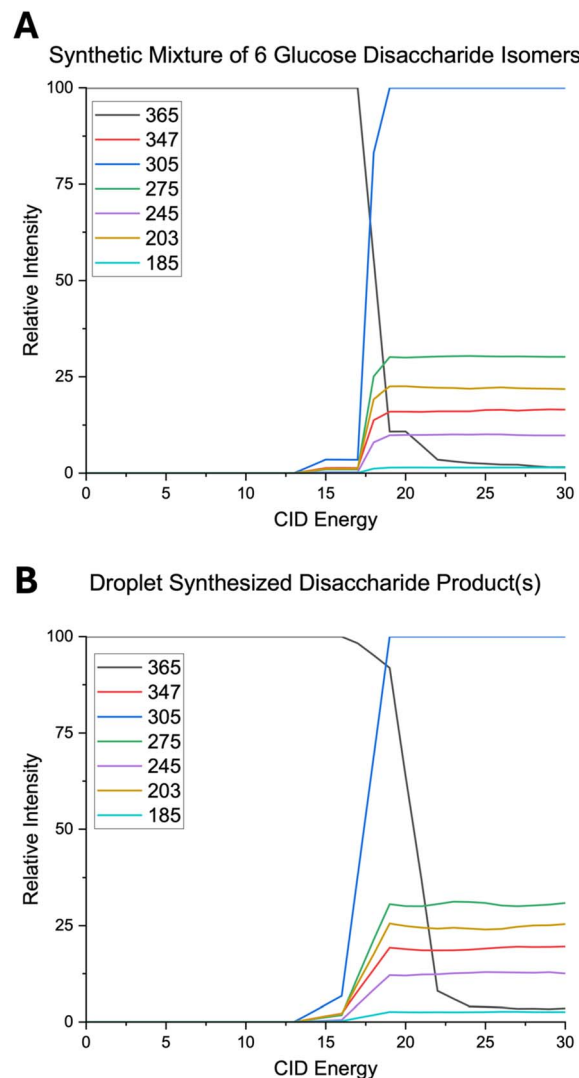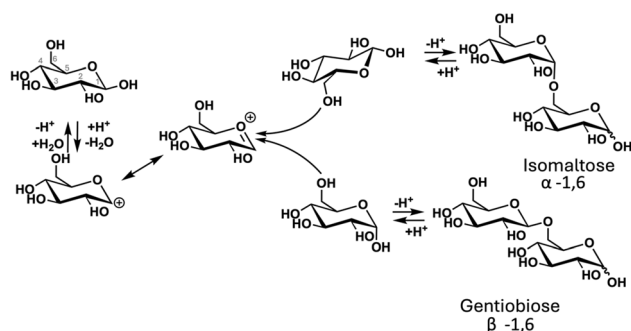
of disaccharides. Other disaccharides and mixtures showed poor matches to the microdroplet product (ESI Fig. S17–S19†).

To further elucidate any differences between the microdroplet synthesized product and the matching disaccharide mixture, breakdown curves were created where the CID energy was varied from nominal values of 0–30 as shown in Fig. 4. A breakdown curve, a set of MS/MS products and intensities recorded over a range of collision energies provides a graphical representation of how the abundances of precursor and fragment ions change with internal energy.[81] Fig. 4 shows strong alignment in product peak intensities, with a maximum 3% difference, and consistent fragmentation onset. The only notable difference is a 2-unit CID difference at the crossover point of *m/z* 365 (precursor ion) and *m/z* 275 (fragment ion). Other disaccharides and mixtures showed poor overlap with the data for the glucose product (Fig. S20 and S21†).

Acid-Catalyzed Glucose Disaccharide formation

Scheme 2 Acid-catalysed glycosylation of glucose. The mechanism for unprotected glucose glycosylation is illustrated as yielding two disaccharides, isomaltose and gentiobiose among other disaccharides. Mechanism adapted from ref. 80.

This mixture of products is suggested to arise *via* microdroplet driven acid catalysis. This is based on literature evidence that microdroplet surfaces can be strongly acidic[82–85] and the agreement of the reaction product distributions with those known to be produced *via* acid catalysis.[80] The acid-catalyzed mechanism depicted in Scheme 2 involves protonation of the C1 hydroxyl group of the glycosyl donor by the acidic microdroplet surface, followed by water loss to form an oxocarbenium ion intermediate, which undergoes nucleophilic attack by the C6 hydroxyl group. This reaction predominantly forms disaccharides with 1,6 linkages like isomaltose and gentiobiose.

The comparison between the microdroplet products and simulated mixture indicates the presence of both α- and β-1,6 linkages, as well as α-1,1, -1,2, -1,3 and -1,4 linkages, with the 1,6 linkages being dominant. The α/β-1,6 glycosidic linkage is likely favored due to the lower steric hindrance of the primary hydroxyl group at C6, making it more accessible for nucleophilic attack.[19] Furthermore, the α-anomeric linkages are preferred over the β isomers due to the anomeric effect[78] with the β-1,6 linkage being less present due to the accessibility of the C6 primary alcohol.

It is well known that the addition of acid can cause further dehydration reactions of monosaccharides. In bulk reactions this leads to products such as hydroxymethylfurfural yet this peak is not observed in the experimental mass spectrum.[17] Oligomerization of glucose is favored under mild acidic conditions high loading concentrations and decreased water activity (ESI Fig. S22 and S23†),[17,19,20] thus enhanced glucose concentrations in the microdroplet combined with short droplet lifetimes and enhanced mass transfer boost effective glucose concentrations and minimize prolonged acidic exposure, reducing side reactions.

Hexose disaccharide quantitation

With the product mixture of the glucose condensation reaction being successfully characterized, the effect of microdroplet size on yield was investigated. Using a pre-charged internal standard, a standard curve was created linking the relative intensity of the disaccharide product to concentration (ESI Note 7 and Fig. S24†). A 250 µL volume of a 10 mM glucose solution was sprayed at 10 µL min⁻¹ for 25 minutes using sonic spray and comparing two silica emitters (250 µm and 50 µm inner diameters). These emitters produce different droplet sizes and, as expected, the smaller droplets are more reactive. The yields are 5.2% (23 µg) and 9.4% yield (43 µg) corresponding to 0.92 µg min⁻¹ emitter and 1.72 µg min⁻¹ emitter for the 250 and 50 micron I.D. respectively. These effects are in line with expected microdroplet mechanisms where smaller droplets provide faster reactions.[59]

Prebiotic implications

The formation of glucose disaccharides like maltose, an energy storage molecule, highlights the potential of microdroplets to facilitate the abiotic synthesis of biologically relevant molecules. Moreover, the ability of pentose sugars, such as xylose, to form disaccharides is significant because structural pentose polymers, like xylans can be found naturally, and represent a previously unexplored link between abiotic chemistry at the origins of life and modern biological systems. The abiotic pathway discussed in this manuscript generates molecules like those known in extant biology to be structural components of cell walls and some identified as sources of metabolic energy.

Furthermore, the stability of sugars in prebiotic environments is a long standing problem in prebiotic chemistry noted by Stanley Miller, as monosaccharides like ribose are highly susceptible to hydrolysis, particularly at elevated temperatures or extreme pH.[86] Disaccharides, in contrast, are significantly more resistant to hydrolysis, with rate constants that are orders of magnitude smaller than those of their monosaccharide counterparts.[87] This increased stability suggests that the formation of disaccharides in microdroplets could serve as a mechanism to preserve sugars in prebiotic environments, allowing them to persist longer and participate in further chemical evolution.

Conclusions

Our data show that the trioses, glyceraldehyde and dihydroxyacetone, form sorbose and fructose when sprayed in water microdroplets. This result follows from the fact that microdroplets containing either glyceraldehyde or dihydroxyacetone gave a covalent product, seen as negative ions of *m/z* 179 and shown by its MS/MS data to correspond to a mixture of deprotonated sorbose and fructose. This study also provides evidence that hexose disaccharides, previously observed in plausible primordial environments, and pentose disaccharides, as demonstrated here for the first time, can form in microdroplets under abiotic conditions. Pentoses and hexoses form disaccharides in microdroplets during their brief flight time from the emitter to the inlet of the mass spectrometer without the need for any additional acid or base. The fragmentation of the glucose disaccharide products showed good agreement with that of the same mixture of disaccharides associated with the

bulk acid-catalyzed glycosylation of glucose. In addition, pentoses dimerize although the exact mixture of isomers produced remains elusive due to the limited availability of pentose disaccharide standards.

These findings support the hypothesis that the air–water interface of aqueous microdroplets, characterized by an acidic and/or basic environment, can serve as a locale for chemistry relevant to the origins of life. Such a mechanism is plausible for abiotic synthesis under conditions like sea spray aerosols and is potentially analogous to the generation of aerosols on ocean worlds like Enceladus where disaccharides might be found.

Data availability

All data on which this publication is based appears either in the main text or in the ESI.† The underlying raw data is available on request to the authors.

Author contributions

All authors contributed to experimental design and data interpretation. DTH and MQE performed the experiments. DTH, MQE, and RGC wrote the manuscript.

Conflicts of interest

There are no conflicts to declare.

Acknowledgements

References

1 H. E. Murrey and L. C. Hsieh-Wilson, *Chem. Rev.*, 2008, **108**, 1708–1731.

2 M. Calvin, *Angew Chem. Int. Ed. Engl.*, 1974, **13**, 121–131.

3 R. Stern and M. J. Jedrzejas, *Chem. Rev.*, 2008, **108**, 5061–5085.

4 A. L. Weber, *Orig. Life Evol. Biosph.*, 2001, **31**, 71–86.

5 A. Butlerow, *Justus Liebigs Ann. Chem.*, 1861, **120**, 295–298.

6 N. W. Gabel and C. Ponnamperuma, *Nature*, 1967, **216**, 453–455.

7 J. B. Lambert, S. A. Gurusamy-Thangavelu and K. Ma, *Science*, 2010, **327**, 623–627.

8 C. Appayee and R. Breslow, *J. Am. Chem. Soc.*, 2014, **136**, 3720–3723.

9 R. Breslow, *Tetrahedron Lett.*, 1959, **1**, 22–26.

10 J. M. Hollis, P. R. Jewell, F. J. Lovas and A. Remijan, *Astrophys. J.*, 2004, **613**, L45–L48.

11 S. L. Widicus Weaver and G. A. Blake, *Astrophys. J.*, 2005, **624**, L33–L36.

12 S. A. Sandford, M. Nuevo, P. P. Bera and T. J. Lee, *Chem. Rev.*, 2020, **120**, 4616–4659.

13 Y. Furukawa, Y. Chikaraishi, N. Ohkouchi, N. O. Ogawa, D. P. Glavin, J. P. Dworkin, C. Abe and T. Nakamura, *Proc. Natl. Acad. Sci. U.S.A.*, 2019, **116**, 24440–24445.

14 G. Cooper, N. Kimmich, W. Belisle, J. Sarinana, K. Brabham and L. Garrel, *Nature*, 2001, **414**, 879–883.

15 L. E. Orgel, *Proc. Natl. Acad. Sci. U.S.A.*, 2000, **97**, 12503–12507.

16 H. M. Pilath, W. E. Michener and R. Katahira, *Energy Fuels*, 2013, **27**, 7560–7568.

17 H. M. Pilath, M. R. Nimlos, A. Mittal, M. E. Himmel and D. K. Johnson, *J. Agric. Food Chem.*, 2010, **58**, 6131–6140.

18 D. H. Ball and J. K. N. Jones, *J. Chem. Soc.*, 1958, **33**, 33–36.

19 A. Thompson, K. Anno, M. L. Wolfrom and M. Inatome, *J. Am. Chem. Soc.*, 1954, **76**, 1309–1311.

20 Z. Li, L. Li, K. R. McKenna, M. Schmidt, P. Pollet, L. Gelbaum, F. M. Fernández, R. Krishnamurthy and C. L. Liotta, *Orig. Life Evol. Biosph.*, 2019, **49**, 225–240.

21 B. T. Burcar, L. M. Barge, D. Trail, E. B. Watson, M. J. Russell and L. B. McGown, *Astrobiology*, 2015, **15**, 509–522.

22 S. Becker, C. Schneider, H. Okamura, A. Crisp, T. Amatov, M. Dejmek and T. Carell, *Nat. Commun.*, 2018, **9**, 163.

23 B. K. D. Pearce, R. E. Pudritz, D. A. Semenov and T. K. Henning, *Proc. Natl. Acad. Sci. U. S. A.*, 2017, **114**, 11327–11332.

24 T. D. Campbell, R. Febrian, J. T. McCarthy, H. E. Kleinschmidt, J. G. Forsythe and P. J. Bracher, *Nat. Commun.*, 2019, **10**, 4508.

25 J. G. Forsythe, S.-S. Yu, I. Mamajanov, M. A. Grover, R. Krishnamurthy, F. M. Fernández and N. V. Hud, *Angew. Chem., Int. Ed.*, 2015, **54**, 9871–9875.

26 K. A. Prather, T. H. Bertram, V. H. Grassian, G. B. Deane, M. D. Stokes, P. J. DeMott, L. I. Aluwihare, B. P. Palenik, F. Azam, J. H. Seinfeld, R. C. Moffet, M. J. Molina, C. D. Cappa, F. M. Geiger, G. C. Roberts, L. M. Russell, A. P. Ault, J. Baltrusaitis, D. B. Collins, C. E. Corrigan, L. A. Cuadra-Rodriguez, C. J. Ebben, S. D. Forestieri, T. L. Guasco, S. P. Hersey, M. J. Kim, W. F. Lambert, R. L. Modini, W. Mui, B. E. Pedler, M. J. Ruppel, O. S. Ryder, N. G. Schoepp, R. C. Sullivan and D. Zhao, *Proc. Natl. Acad. Sci. U. S. A.*, 2013, **110**, 7550–7555.

27 H. Sharma, M. M. Hedman and S. Vahidinia, *Planet. Sci. J.*, 2023, **4**, 116.

28 C. P. McKay, A. D. Anbar, C. Porco and P. Tsou, *Astrobiology*, 2014, **14**, 352–355.

29 C. P. McKay, C. C. Porco, T. Altheide, W. L. Davis and T. A. Kral, *Astrobiology*, 2008, **8**, 909–919.

30 D. T. Holden, N. M. Morato and R. G. Cooks, *Proc. Natl. Acad. Sci. U.S.A.*, 2022, **119**, e2212642119.

31 H. Chen, R. Wang, T. Chiba, K. Foreman, K. Bowen and X. Zhang, *J. Am. Chem. Soc.*, 2024, **146**, 10979–10983.

32 E. Gnanamani, X. Yan and R. N. Zare, *Angew. Chem., Int. Ed.*, 2020, **59**, 3069–3072.

33 Z. Wei, Y. Li, R. Graham Cooks and X. Yan, *Annu. Rev. Phys. Chem.*, 2020, **71**, 31–55.

34 X. Yan, R. M. Bain and R. G. Cooks, *Angew. Chem., Int. Ed.*, 2016, **55**, 12960–12972.

35 X. Yan, *Int. J. Mass Spectrom.*, 2021, **468**, 116639.

36 K. J. Vannoy, M. Q. Edwards, C. Renault and J. E. Dick, *Annu. Rev. Anal. Chem.*, 2024, **17**, 149–171.

37 C. M. Dobson, G. B. Ellison, A. F. Tuck and V. Vaida, *Proc. Natl. Acad. Sci. U.S.A.*, 2000, **97**, 11864–11868.

38 A. Tuck, *Surv. Geophys.*, 2002, **23**, 379–409.

39 L. Qiu, Z. Wei, H. Nie and R. G. Cooks, *ChemPhysChem*, 2021, **86**, 1362–1365.

40 K. D. Judd, S. W. Parsons, D. B. Eremin, V. V. Fokin and J. M. Dawlaty, *Chem. Sci.*, 2024, **15**, 8346–8354.

41 K. H. Huang, Z. Wei and R. G. Cooks, *Chem. Sci.*, 2021, **12**, 2242–2250.

42 P. Basuri, L. E. Gonzalez, N. M. Morato, T. Pradeep and R. G. Cooks, *Chem. Sci.*, 2020, **11**, 12686–12694.

43 H. Wei, E. P. Vejerano, W. Leng, Q. Huang, M. R. Willner, L. C. Marr and P. J. Vikesland, *Proc. Natl. Acad. Sci. U. S. A.*, 2018, **115**, 7272–7277.

44 M. de la Puente and D. Laage, *J. Am. Chem. Soc.*, 2023, **145**, 25186–25194.

45 H. Xiong, J. K. Lee, R. N. Zare and W. Min, *J. Phys. Chem. Lett.*, 2020, **11**, 7423–7428.

46 H. Hao, L. Ruiz Pestana, J. Qian, M. Liu, Q. Xu and T. Head-Gordon, *Wiley Interdiscip. Rev.: Comput. Mol. Sci.*, 2022, **13**, e1639.

47 A. M. Deal, R. J. Rapf and V. Vaida, *J. Phys. Chem. A*, 2021, **125**, 4929–4942.

48 L. Qiu and R. G. Cooks, *Proc. Natl. Acad. Sci. U.S.A.*, 2024, **121**, e2309360120.

49 W. Wang, L. Qiao, J. He, Y. Ju, K. Yu, G. Kan, C. Guo, H. Zhang and J. Jiang, *J. Phys. Chem. Lett.*, 2021, **12**, 5774–5780.

50 I. Nam, J. K. Lee, H. G. Nam and R. N. Zare, *Proc. Natl. Acad. Sci. U. S. A.*, 2017, **114**, 12396–12400.

51 Y. Ju, H. Zhang, W. Wang, Q. Liu, K. Yu, G. Kan, L. Liu and J. Jiang, *J. Phys. Chem. Lett.*, 2022, **13**, 567–573.

52 I. Nam, H. G. Nam and R. N. Zare, *Proc. Natl. Acad. Sci. U. S. A.*, 2018, **115**, 36–40.

53 A. D. Castañeda, Z. Li, T. Joo, K. Benham, B. T. Burcar, R. Krishnamurthy, C. L. Liotta, N. L. Ng and T. M. Orlando, *Sci. Rep.*, 2019, **9**, 13527.

54 Y. Ju, H. Zhang, X. Wang, Y. Liu, Y. Yang, G. Kan, K. Yu and J. Jiang, *J. Colloid Interface Sci.*, 2023, **634**, 535–542.

55 J. S. Bhanot, K. C. Fabijanczuk, A. M. Abdillahi, H.-C. Chao, N. J. Pizzala, F. A. Londry, E. T. Dziekonski, J. W. Hager and S. A. McLuckey, *Int. J. Mass Spectrom.*, 2022, **478**, 116874.

56 G. R. D. Prabhu, E. R. Williams, M. Wilm and P. L. Urban, *Nat. Rev. Methods Primers*, 2023, **3**, 23.

57 J. N. Smith, R. C. Flagan and J. L. Beauchamp, *J. Phys. Chem. A*, 2002, **106**, 9957–9967.

58 A. Hollerbach, D. Logsdon, K. Iyer, A. Li, J. A. Schaber and R. G. Cooks, *Analyst*, 2017, **143**, 232–240.

59 B. M. Marsh, K. Iyer and R. G. Cooks, *J. Am. Soc. Mass Spectrom.*, 2019, **30**, 2022–2030.

60 A. Hirabayashi, M. Sakairi and H. Koizumi, *Anal. Chem.*, 1995, **67**, 2878–2882.

61 A. Özdemir, J. L. Lin, Y. S. Wang and C. H. Chen, *RSC Adv.*, 2014, **4**, 61290–61297.

62 H. Nie, Z. Wei, L. Qiu, X. Chen, D. T. Holden and R. G. Cooks, *Chem. Sci.*, 2020, **11**, 2356–2361.

63 T. P. Roche, D. M. Fialho, C. Menor-Salván, R. Krishnamurthy, G. B. Schuster and N. V. Hud, *Chem.–Eur. J.*, 2023, **29**, e202203036.

64 R. E. March and C. J. Stadey, *Rapid Commun. Mass Spectrom.*, 2005, **19**, 805–812.

65 E. Amoah, T. Sahraeian, A. Seth and A. K. Badu-Tawiah, *Analyst*, 2024, **149**, 5504–5517.

66 V. F. Taylor, R. E. March, H. P. Longerich and C. J. Stadey, *Int. J. Mass Spectrom.*, 2005, **243**, 71–84.

67 B. Domon and C. E. Costello, *Glycoconj. J.*, 1988, **5**, 397–409.

68 M. Li, C. Boothby, R. E. Continetti and V. H. Grassian, *J. Am. Chem. Soc.*, 2023, **145**, 22317–22321.

69 M. Li, S. Yang, M. Rathi, S. Kumar, C. S. Dutcher and V. H. Grassian, *Chem. Sci.*, 2024, **15**, 13429–13441.

70 P. Kim and R. E. Continetti, *ACS Earth Space Chem.*, 2021, **5**, 2212–2222.

71 S. J. Angyal, *Glycoscience*, 2001, **1**, 1–14.

72 J. P. Heindel, R. A. LaCour and T. Head-Gordon, *Nat. Commun.*, 2024, **15**, 3670.

73 N. B. Cech and C. G. Enke, *Mass Spectrom. Rev.*, 2001, **20**, 362–387.

74 S. H. Giese, A. Belsom, L. Sinn, L. Fischer and J. Rappsilber, *Anal. Chem.*, 2019, **91**, 2678–2685.

75 H.-S. Nguan and C.-K. Ni, *J. Phys. Chem. A*, 2022, **126**, 8799–8808.

76 E. V. da Costa, A. S. P. Moreira, F. M. Nunes, M. A. Coimbra, D. V. Evtuguin and M. R. M. Domingues, *Rapid Commun. Mass Spectrom.*, 2012, **26**, 2897–2904.

77 K. D. Swanson, S. E. Spencer and G. L. Glish, *J. Am. Soc. Mass Spectrom.*, 2016, **28**, 1030–1035.

78 A. V. Demchenko, *Handbook of Chemical Glycosylation: Advances in Stereoselectivity and Therapeutic Relevance*, Wiley-VCH, Weinheim, 2008, pp. 1–27.

79 B. J. Bythell, M. T. Abutokaikah, A. R. Wagoner, S. Guan and J. M. Rabus, *J. Am. Soc. Mass Spectrom.*, 2017, **28**, 688–703.

80 N. Li, Z. Wang, T. Qu, J. Kraft, J. H. Oh, J. P. Van Pijkeren, G. W. Huber and X. Pan, *Green Chem.*, 2019, **21**, 2686–2698.

81 S. A. McLuckey, G. L. Glish and R. G. Cooks, *Int. J. Mass Spectrom. Ion Phys.*, 1981, **39**, 219–230.

82 Z. Song, C. Zhu, K. Gong, R. Wang, J. Zhang, S. Zhao, Z. Li, X. Zhang and J. Xie, *J. Am. Chem. Soc.*, 2024, **146**, 10963–10972.

83 K. Gong, J. Ao, K. Li, L. Liu, Y. Liu, G. Xu, T. Wang, H. Cheng, Z. Wang, X. Zhang, H. Wei, C. George, A. Mellouki, H. Herrmann, L. Wang, J. Chen, M. Ji, L. Zhang and J. S. Francisco, *Proc. Natl. Acad. Sci. U.S.A.*, 2023, **120**, e2219588120.

84 Y. L. S. Tse, C. Chen, G. E. Lindberg, R. Kumar and G. A. Voth, *J. Am. Chem. Soc.*, 2015, **137**, 12610–12616.

85 M. Girod, E. Moyano, D. I. Campbell and R. G. Cooks, *Chem. Sci.*, 2011, **2**, 501–510.

86 R. Larralde, M. P. Robertson and S. L. Miller, *Proc. Natl. Acad. Sci. U.S.A.*, 1995, **92**, 8158–8160.

87 R. Wolfenden and Y. Yuan, *J. Am. Chem. Soc.*, 2008, **130**, 7548–7549.